

Supplemental Information for “Uranium incorporation into aluminum-substituted ferrihydrite during iron(II)-induced transformation”

This supplement includes detailed information on analyses conducted for the paper, including: X-ray scattering experiments of ferrihydrite precursors, X-ray powder diffractograms and Rietveld analysis of goethite transformation products, and EXAFS fitting and analysis. Additionally, data are presented from total X-ray scattering experiments and X-ray powder diffraction, and Rietveld analysis of the powder diffractograms is also detailed. A linear combination fitting procedure was used to distinguish between adsorbed U(VI) and incorporated U(V) in U EXAFS spectra, and between goethite and ferrihydrite in Fe EXAFS spectra. “Standard” components used in linear combination fits were described using “shell-by-shell” fitting of EXAFS spectra from structural models. The Supplemental Information also contains supplemental Fe K-edge EXAFS linear combination fits, and a discussion of uncertainty estimates of EXAFS linear combination fitting.

S1. Total X-ray scattering and pair distribution function analysis

Total X-ray scattering and pair distribution function analysis were performed on dried synthetic Al-ferrihydrite slurry samples with 0-20% Al substitution for Fe, in a manner identical to that described in Cismasu et al. ¹. X-ray diffractograms showing two-line ferrihydrite are shown in Figure S1, and pair distribution functions are shown in Figure S2.

S2. X-ray powder diffractograms

High-resolution synchrotron X-ray powder diffraction was used to identify crystalline solid phases in the synthetic U-bearing iron/aluminum oxide samples. The diffractograms are shown in Figure S3. Rietveld analysis of XRD patterns is discussed below.

S2.1. Rietveld analysis

Rietveld analysis on goethite X-ray diffraction patterns was performed using the EXPGUI software interface ² to the Generalized Structure Analysis System (GSAS) ³. Backgrounds were fit using a shifted Chebyshev polynomial with 16-18 terms. Lattice parameters, isotropic thermal motion (UIISO), and Lorentzian peak shape (isotropic and anisotropic) were included in the refinement. Instrument-specific Gaussian broadening (U, V, W) and zero-shift were determined from fitting a LaB₆ standard diffraction pattern. In some cases, samples required correction for preferential orientation—this was likely due to background scattering from residual ferrihydrite, but may have been due to actual oriented grains.

S3. Uranium L₃-edge and Iron K-edge EXAFS normalization and fitting

S3.1. Calibration, averaging, and normalization of EXAFS spectra

Energy calibration was achieved using simultaneous collection of an in-line metal foil in transmission geometry. A Y foil was used for energy calibration for U L₃-edge and a Fe foil used for Fe K-edge. The first peak in the first derivative of the metal foil XAS spectrum was calibrated to 17038.4 eV for Y and 7111.0 eV for Fe. The co-collected unknown XAS spectra were then referenced against the standard spectrum. Calibration was performed using the SixPack software package ⁴.

In cases where data were collected using a multi-element solid state detector, each individual channel was inspected for data quality and removed if there were obvious data quality issues (such as a Bragg peak, poor signal-to-noise, etc.) Channels with good data were summed to obtain each individual spectrum. Multiple (usually 2-6) spectra were averaged to improve data quality. Averaging was also performed using the SixPack software package ⁴.

S3.1.1. Uranium L₃-edge EXAFS normalization parameters

After averaging, spectra were normalized to a total absorption of unity (as defined by the post-edge envelope), and fit using the Athena data normalization and analysis package ⁵. For U L₃-edge EXAFS, the background was subtracted using pre-edge linear range of -120 to -65 eV (relative to E₀) and a linear post-edge region of 100 to 800 eV (relative to E₀). E₀ was set at the first-derivative peak of the XAS spectrum (ranging from ~17,171 eV to ~17,174 eV, with a typical value being ~17,172 eV). A spline function was used to describe the absorption envelope using a range of $k=1.3$ to $k=14 \text{ \AA}^{-1}$, and a spline (background removal) k -weight of 2. The spline function had an r-

background (“Rbkg” parameter) of 1.0 to remove low frequencies corresponding to non-physical interatomic distances.

The U L₃-edge EXAFS spectra were Fourier transformed over a k -range of $k=3$ to 11 \AA^{-1} , after application of a Kaiser-Bessel windowing function with a Δk of 3 to smooth the EXAFS function.

S3.1.2. Iron K-edge EXAFS normalization parameters

For Fe K-edge EXAFS, E_0 was set at 7,112 eV, and the spline r-background parameter set to 0.9-1.0. Background subtraction was accomplished using a pre-edge range of -150 to -30 eV and a post-edge linear range of 150 to 825 eV. A spline range of $k=1.3$ to $k=14.8 \text{ \AA}^{-1}$ and k -weight of 2 was used to isolate the EXAFS (χ) function.

The Fe K-edge EXAFS spectra were Fourier transformed over a k -range of $k=3$ to 13.5 \AA^{-1} , after application of a Kaiser-Bessel windowing function with a Δk of 2 to smooth the EXAFS function.

S3.2. “Shell-by-shell” fitting of incorporated U and adsorbed U EXAFS standard spectra

“Shell-by-shell” fitting of U L₃-edge EXAFS spectra (for linear combination fits, see below) was conducted using the Athena software package^{5,6} and FEFF 8.4 or FEFF 6⁷. The adsorbed U spectrum was fit in k -space, R-space, and q-space with a k -range of 3 to 13.5 \AA^{-1} , an R range of 1.0 to 3.6 \AA , and a fit k -weight of 3. The Fourier transform and inverse Fourier transform used a Hanning function for windowing, with a Δk of 3 and a Δr of 0.1 for smoothing. The incorporated U(V) spectrum was fit in k -space, R-space, and q-space with a k -range of 3.34 to 13 \AA^{-1} , an R range of 0.8 to 4.5 \AA , and fit k -weights of 1, 2, and 3. The Fourier transform and inverse Fourier

transform again used a Hanning function for windowing, with a Δk of 2 and a Δr of 0.1 for smoothing.

The adsorbed uranyl spectrum was dominated by axial and equatorial O atoms at ~ 1.8 Å and ~ 2.3 - 2.5 Å, respectively, as well as Fe at ~ 3.4 - 3.5 Å, consistent with previous reports⁸. The incorporated U(V) spectrum was dominated by O atoms at 2.12 Å and Fe at 3.25 Å and 3.64 Å; the relatively longer U-O distance and relatively shorter U-Fe distance of 3.25 Å distinguish the incorporated U(V) spectrum from that of adsorbed uranyl. The fitting results for incorporated U(V) are similar to those observed by e.g., Boland et al.⁹ and Nico et al.¹⁰. Tabulated results for the shell-by-shell fitting are given in Table S1.

S3.3. EXAFS linear combination fitting

After normalization, U L₃-edge EXAFS were fit using the linear combination fitting data analysis routine of the Athena⁵. Standards used in the fits were adsorbed uranyl and incorporated U(V) (described in Section S3.2). Fits were performed in k -space using a range of 3 to 11 Å⁻¹, and fit results were constrained such that components (reference spectra) had fitting coefficients between 0 and 1 (i.e., no negative component coefficients). Components were not constrained to sum to 1 in the fitting software itself; instead, the sum of the coefficients of all components was normalized to unity after the linear combination fit. This method yielded lower fit residuals than forcing the fit components to sum to unity as part of the Athena fitting algorithm. However, both methods resulted in similar coefficients for the linear combination fits, after normalization.

Iron K-edge EXAFS spectra were also fit using ferrihydrite and goethite standard component spectra using the linear combination fitting data analysis routine of the Athena software package. Fits were in k -space, and the fit range was $k=3$ to 13 Å⁻¹. Fitting constraints (no negative components) and normalization (sum of coefficients normalized to unity) were identical to the

procedure used for U L₃-edge EXAFS analysis, above. Example Fe K-edge EXAFS spectra and fits are given in Figure S5.

S3.4. Linear combination fitting uncertainty estimates

Uncertainty resulting from data quality was estimated by linear combination fitting of individual EXAFS spectra that constitute each averaged spectrum (see Section B3.1). The standard deviation of these replicate linear combination fitting results were generally $\pm 1-5\%$. Additionally, uncertainty from choice of linear combination fitting parameters was estimated by repeated fitting after slight variation in normalization and fitting parameters such as spline range, spline low-frequency filtering strength (r-background), and fitting range. The choice of parameters accounted for at most $\pm 5-10\%$ variation in the linear combination fitting results. Therefore, the composite uncertainty associated with EXAFS linear combination fitting estimates is approximately $\pm 5-15\%$. Even 15% is a conservative estimate of uncertainty, given that 5% is an upper bound of the standard deviation of the replicate fits, and 10% is the highest observed change in results upon parameter variation; most spectra exhibited approximately $\pm 5-10\%$ variation in linear combination fitting results, depending chiefly on the choice of normalization and fitting parameters.

References

1. A. C. Cismasu, F. M. Michel, J. F. Stebbins, C. Levard, and G. E. Brown Jr., *Geochimica et Cosmochimica Acta*, 2012, **92**, 275–291.
2. B. Toby, *J. Appl. Crystallogr.*, 2001, **34**, 210–213.
3. A. C. Larson and R. B. Von Dreele, *GSAS*, Los Alamos National Laboratory, 2000.
4. S. M. Webb, *Physica Scripta*, 2005, 1011.
5. B. Ravel and M. Newville, *Journal of Synchrotron Radiation*, 2005, **12**, 537–541.
6. B. Ravel, *Journal of Synchrotron Radiation*, 2001, **8**, 314–316.
7. A. L. Ankudinov, J. J. Rehr, and S. D. Conradson, *Phys. Rev. B*, 1998, **58**, 7565–7576.
8. J. Bargar, R. Reitmeyer, and J. Davis, *Environ. Sci. Technol.*, 1999, **33**, 2481–2484.
9. D. D. Boland, R. N. Collins, T. E. Payne, and T. D. Waite, *Environ. Sci. Technol.*, 2011, **45**, 1327–1333.
10. P. S. Nico, B. D. Stewart, and S. Fendorf, *Environ. Sci. Technol.*, 2009, **43**, 7391–7396.

Tables

Table S1. Uranium L₃-edge EXAFS shell-by-shell fitting results for synthetic U-bearing solids. Uranyl was adsorbed on ferrihydrite or incorporated into goethite in order to obtain reference spectra.

	Coordination number	Distance (Å)	σ^2	ΔE_0 (eV)
U adsorbed on Fe				
U-O _{axial}	2.00*	1.81 (\pm 0.02)	0.003 (\pm 0.001)	5.49 (\pm 4.14)
U-O _{axial} MS	2.00†	3.64†	0.005†	5.49†
U-O _{equatorial, 1}	3.21 (\pm 0.91)‡	2.32 (\pm 0.04)	0.007 (\pm 0.004)	5.49†
U-O _{equatorial, 2}	2.79 (\pm 0.91)‡	2.49 (\pm 0.07)	0.008†	5.49†
U-Fe	1.39†	3.48 (\pm 0.10)	0.015 (\pm 0.012)	5.49†
U-C	2.27 (\pm 2.56)	2.90 (\pm 0.08)	0.009†	5.49†
U(V) in goethite				
U-O _{axial, adsorbed}	0.6*	1.80*	0.006 (\pm 0.006)	9.05†
U-O _{incorporated}	5.5*	2.18 (\pm 0.03)	0.013 (\pm 0.002)	9.05 (\pm 3.00)
U-O _{equatorial, ads}	3.0†	2.45 (\pm 0.05)	0.006 (\pm 0.003)	9.05†
U-O _{axial} MS	1.2†	3.59†	0.011†	9.05†
U-Fe _{incorporated, 1}	4.0*	3.25 (\pm 0.02)	0.015 (\pm 0.003)	9.05†
U-Fe _{incorporated, 2}	3.0*	3.64 (\pm 0.02)	0.013 (\pm 0.004)	9.05†

* Parameter was set as a constant value in the fit.

† Parameter was defined as a function of other parameters in the fit.

‡ Parameter was constrained to sum to U-O_{equatorial, total} = 6 in the fit.

Figures

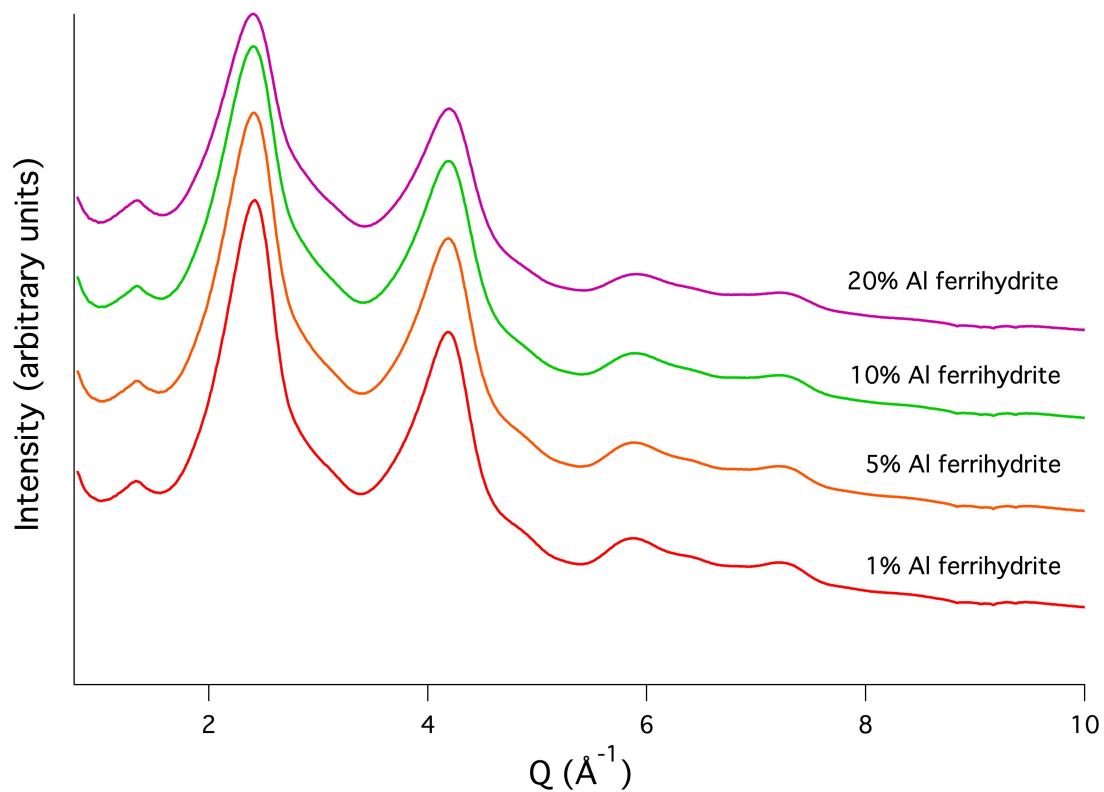


Figure S1. X-ray diffractograms of initial Al-ferrihydrite slurry (1-20 mol% Al substituted for Fe), with the two broad diffraction peaks centered at $Q \sim 2.4 \text{ \AA}^{-1}$ and $Q \sim 4.1 \text{ \AA}^{-1}$ confirming two-line ferrihydrite mineralogy.

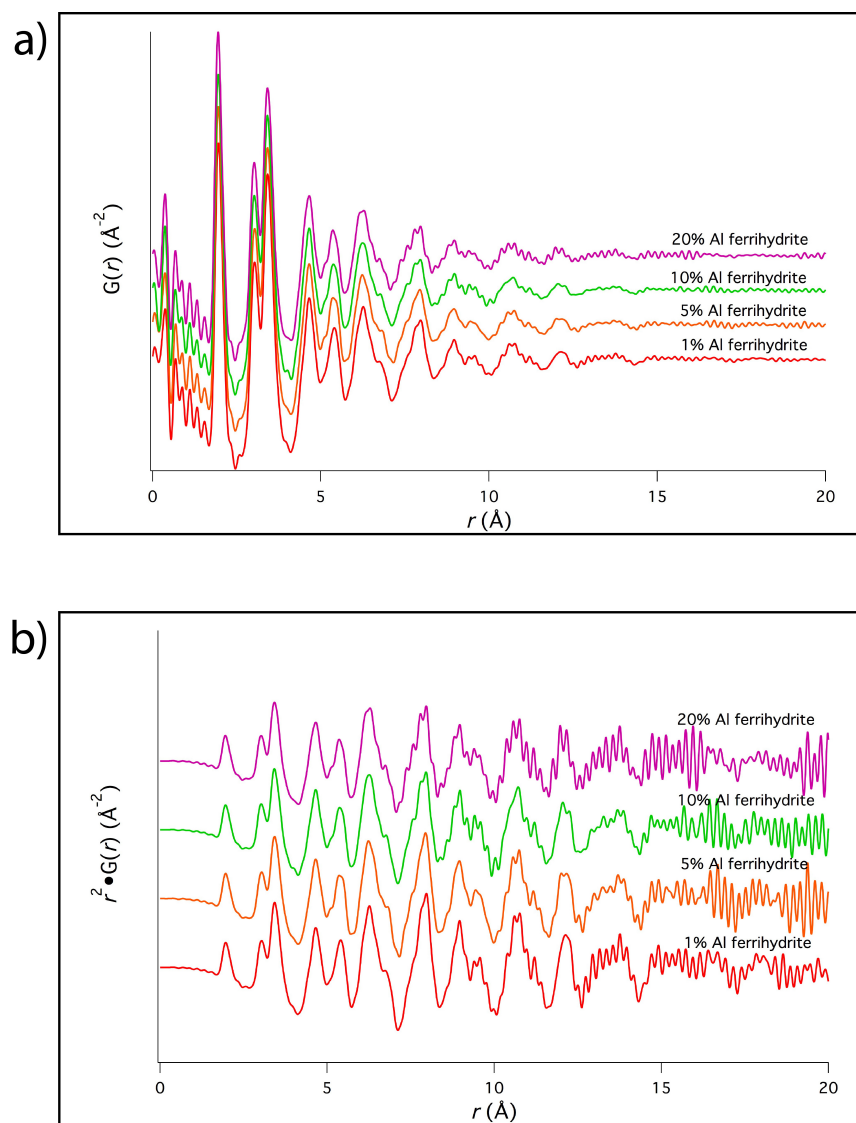


Figure S2. High energy total scattering pair distribution function of two-line Al-ferrihydrate slurry (1-20 mol% Al substituted for Fe), a) unweighted, and b) weighted by R^2 to accentuate the later parts of the wave (showing decay in approximately the same range). Decreasing coherent scattering domain size can be inferred from intensity loss with increasing Al content rather than differences in wave decay, but interpretation of the intensity is confounded by other factors (e.g., lower scattering cross-section of Al).

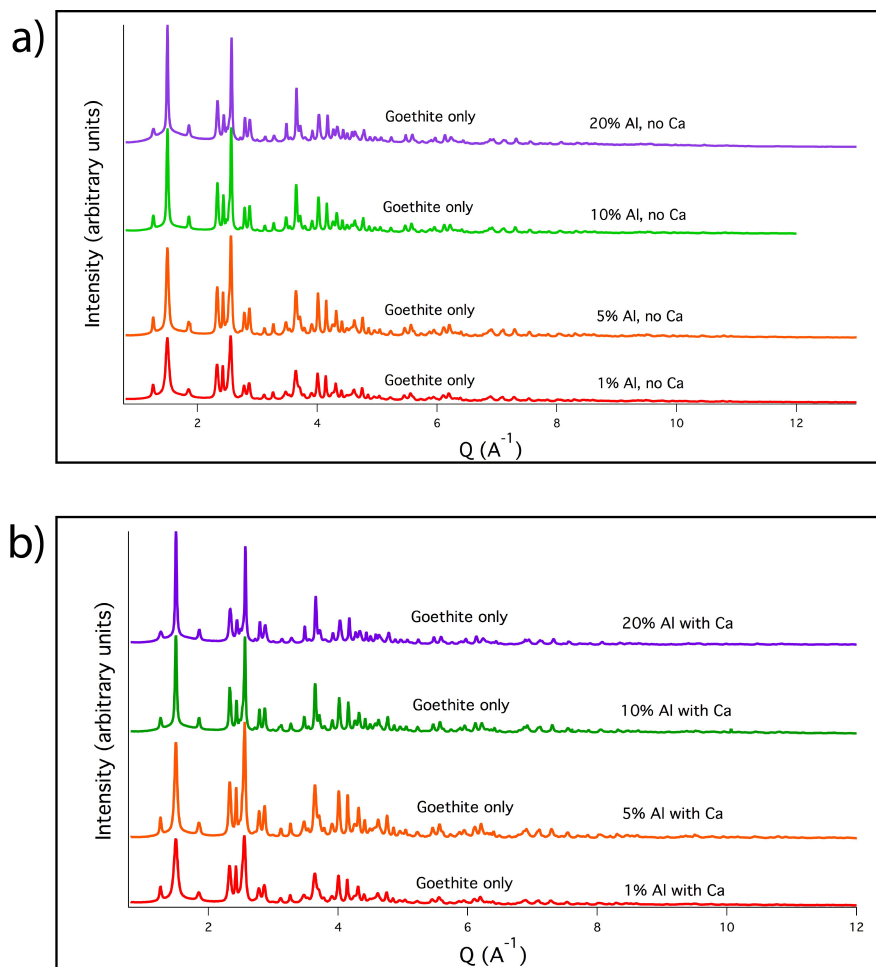


Figure S3. Crystalline solid phases identified with high-resolution powder diffraction, resulting from U(VI) ($[U_{\text{initial}}]=10 \mu\text{M}$) reacted with Al-ferrihydrite slurry (0-20 mol% Al substituted for Fe), 0.3 mM Fe(II), 3.8 mM carbonate, and (a) 0 mM Ca or (b) 4 mM Ca, at pH 7.0.

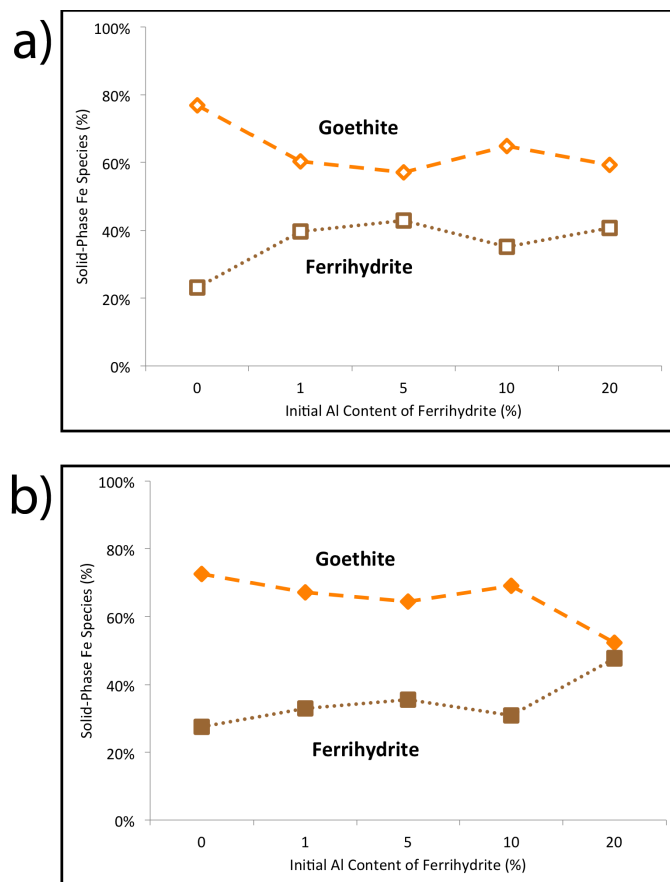


Figure S4. Solid phase Fe speciation from Fe K-edge EXAFS linear combination fits, as a function of initial Al content of ferrihydrite slurry (0-20 mol% Al substitution for Fe), after reaction with 10 μM initial $\text{U(VI)}_{(aq)}$, 0.3 mM Fe(II), 3.8 mM carbonate, and a) 0 mM Ca or b) 4 mM Ca, at pH 7.0. Goethite is the major transformation product of ferrihydrite, but declines with increasing Al content. Linear combination fitting EXAFS percentages are shown for each component: goethite (yellow circles), and ferrihydrite (brown squares).

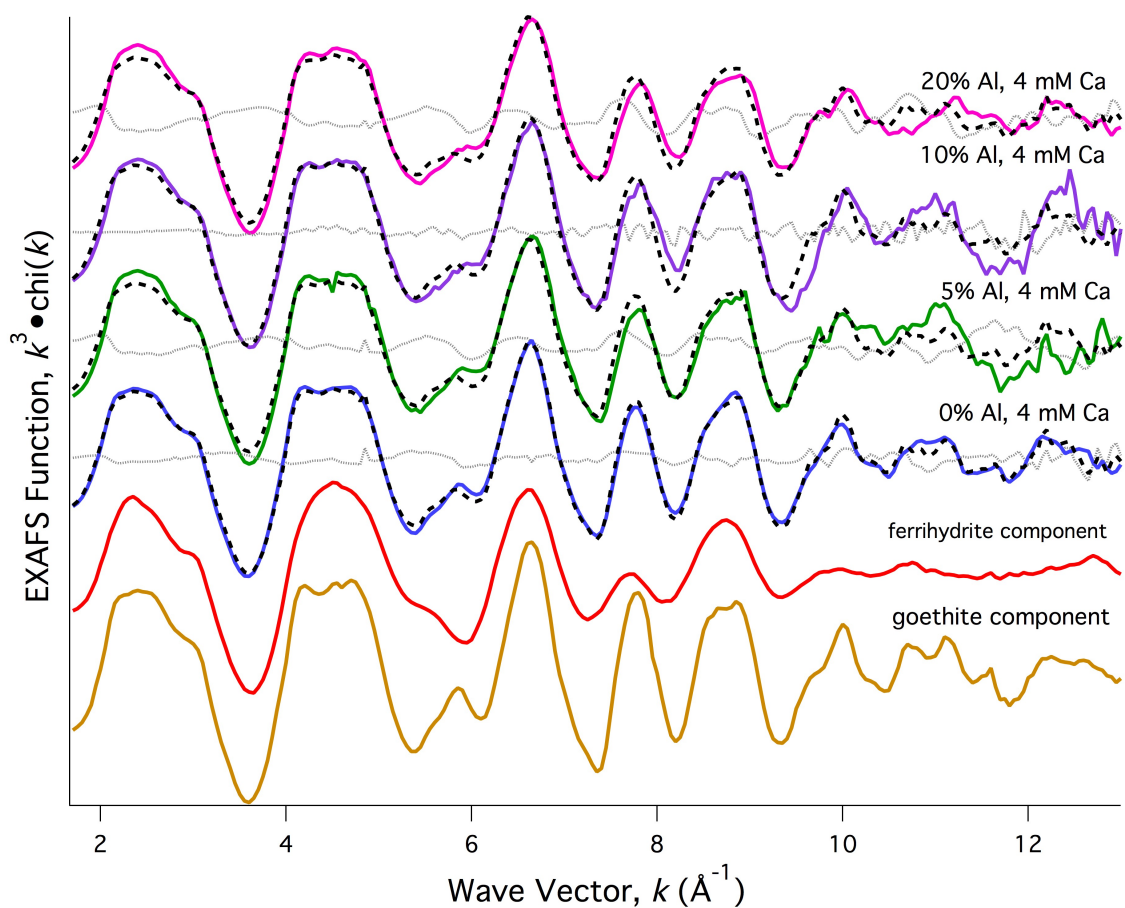


Figure S5. EXAFS linear combination fitting results for k^3 -weighted Fe K-edge EXAFS spectra for Al-ferrihydrite (0-20 mol% Al substituted for Fe) reacted with 10 μM U(VI), 0.3 mM Fe(II), 3.8 mM carbonate, and 0 mM Ca, at pH 7.0. Data (colored lines), fitting components (goethite, ferrihydrite), linear combination fits (black dotted lines), and residuals (light grey dotted lines) are shown.